

AN ESTIMATE OF CHROMOSPHERIC HEATING BY ACOUSTIC WAVES

M. SOBOTKA¹, M. ŠVANDA^{1,2}, J. JURČÁK¹, P. HEINZEL¹,
D. DEL MORO³ and F. BERRILLI³

¹*Astronomical Institute, Academy of Sciences of the Czech Republic (v.v.i.),
Fričova 298, CZ–25165 Ondřejov, Czech Republic*

²*Astronomical Institute, Charles University in Prague,
Faculty of Mathematics and Physics,*

V Holešovičkách 2, CZ–18000 Prague 8, Czech Republic

³*Department of Physics, University of Roma Tor Vergata,
via della Ricerca Scientifica 1, I–00133 Rome, Italy*

Abstract. Several mechanisms may heat the solar chromosphere: acoustic waves, magnetoacoustic waves (slow, fast, and Alfvén waves), and small-scale magnetic reconnections. Based on observations in the Ca II 854.2 nm line, the contribution of acoustic waves to the heating of quiet and plage regions in the chromosphere is discussed. The energy released by radiative losses is compared with the energy deposited by acoustic waves. Radiative losses are computed using a grid of six semi-empirical models VAL A–F. The deposited acoustic flux is calculated using power spectra of Doppler oscillations measured in the Ca II line core. The comparison shows that the spatial correlation of maps of radiative losses and acoustic flux is 70 %. The deposited acoustic flux provides at least 25–30 % of the energy radiated in the quiet chromosphere and 50 % in plage regions.

Key words: Sun - chromosphere - heating - waves

1. Introduction

Analysis of chromospheric lines (typically of Ca II, Mg II, and H) shows that the temperature in the chromosphere is higher than that on the top of the photosphere. There are several candidate mechanisms for the chromospheric heating: acoustic waves, magnetoacoustic waves (slow, fast, and Alfvén waves), and small-scale magnetic reconnections (Stix 2004). Acoustic waves, generated by turbulent convection on the bottom of the photosphere, may transport enough energy. However, Bel and Leroy (1977) have shown that waves with frequencies $\nu < \nu_{\text{ac}} = \gamma g / (4\pi c_s) = 5.2$ mHz cannot propagate higher into the atmosphere. The limiting frequency ν_{ac} is called the

acoustic cutoff and depends on the adiabatic coefficient $\gamma = 5/3$, gravitational acceleration g , and the sound speed c_s . The situation changes in the presence of magnetic field. Acoustic waves convert, still in the photosphere, into slow and fast magnetoacoustic waves (see e.g. Stangalini *et al.* 2011) and the inclined magnetic field provides “portals” through which low-frequency magnetoacoustic waves can propagate into the chromosphere (Jefferies *et al.* 2006). We have shown (Sobotka *et al.* 2013) that the chromosphere above a light bridge, located inside a large pore, can be heated by acoustic waves thanks to that mechanism. In the present work we attempt to estimate the contribution of acoustic energy flux to the chromospheric heating in quiet and plage regions.

2. Observations and data reduction

The active region NOAA 11005 was observed on 15 October 2008 from 16:34 to 17:43 UT with the Interferometric Bidimensional Spectrometer (IBIS, Cavallini 2006) attached to the Dunn Solar Telescope. The slowly decaying pore, located at the heliocentric angle $\vartheta = 23^\circ$ during our observation, led a bipolar active region, in which the following magnetic polarity was too weak to produce sunspots or pores. A weak chromospheric plage with the same magnetic polarity as the pore was located at the eastern edge of the field of view (FOV). The IBIS dataset consists of 80 sequences, each containing a full Stokes (I, Q, U, V) 21-point scan of the Fe I 617.33 nm line and a 21-point I -scan of the Ca II 854.2 nm infrared line. The wavelength distance between the spectral points for the Fe I line is 2.0 pm and 6.0 pm for the Ca II line. The exposure time for each image was set to 80 ms and each sequence took 52 s to complete, thus setting the time resolution. The pixel scale of the images was 0.167 arcsec.

According to Cauzzi *et al.* (2008), the wings at ± 60 pm of the infrared Ca II 854.2 nm line sample the middle photosphere at the typical height $h \simeq 250$ km above the $\tau_{500} = 1$ level, while the centre of this line is formed in the middle chromosphere at $h \simeq 1200\text{--}1400$ km. Doppler shifts of the line profile were measured using the double-slit method (Garcia *et al.* 2010), consisting in the minimization of difference between intensities measured in the opposite wings of the line. The wavelength points were selected in the inner wings near the line core, where the effective formation height in the atmosphere is approximately 1000 km. The sensitivity of the Doppler

velocity measurement is 53 m s^{-1} and the reference zero is defined as a time- and space-average of all measurements. An alternative measurement of Doppler shifts based on a parabolic fit of the central part of the Ca II profile formed at $h \simeq 1400 \text{ km}$ gave practically identical results. Spectral power density $P_v(\nu, x, y)$ of Doppler oscillations in the FOV was calculated in the frequency range 1–9 mHz using standard Fourier analysis. Given the length of the time series and the sampling rate, the frequency resolution is 0.24 mHz. We applied the Stokes inversion code based on response functions (SIR, Ruiz Cobo and del Toro Iniesta 1992) on the Fe I Stokes profiles to retrieve the magnetic field vector in the photosphere. The field was assumed to be constant with height to keep the number of free parameters as low as possible. See Sobotka *et al.* (2013) for the detailed description of observations and data reduction.

3. Results

The energy released by radiation from the chromosphere is characterized by net radiative cooling rates (radiative losses), which, on the other hand, indicate the amount of non-radiative heating that sustains the temperature at a given height in the atmosphere. To calculate them, we used a grid of six semi-empirical models A–F published by Vernazza *et al.* (1981). Model A corresponds to a dark point in the intranetwork, model B characterizes an average intranetwork area, model C an average quiet Sun, and model D an average network. Models E and F describe bright and very bright network elements, respectively. Synthetic profiles of the Ca II 854.2 nm line were computed for each model using a non-LTE atmospheric code based on the MALI technique (Rybicki and Hummer 1992). Models A–F were assigned to each point in the FOV according to the best match of the synthetic to the observed profiles averaged in time. The same code was used to compute for each model (and the corresponding points in the FOV) the net radiative cooling rates for the lines Ca II *K*, *H* and the infrared triplet, hydrogen lines, and hydrogen continua. The total Ca II radiative losses were integrated in the height range 660–2000 km. The radiative losses of hydrogen are negligible in this range. The contribution of the Mg II *k*, *h* lines was approximated by a multiplicative factor of 1.3 (Vernazza *et al.* 1981). This way we obtained a map of radiative losses in the FOV that covers a part of the chromospheric plage and quiet chromosphere (Fig. 1b).

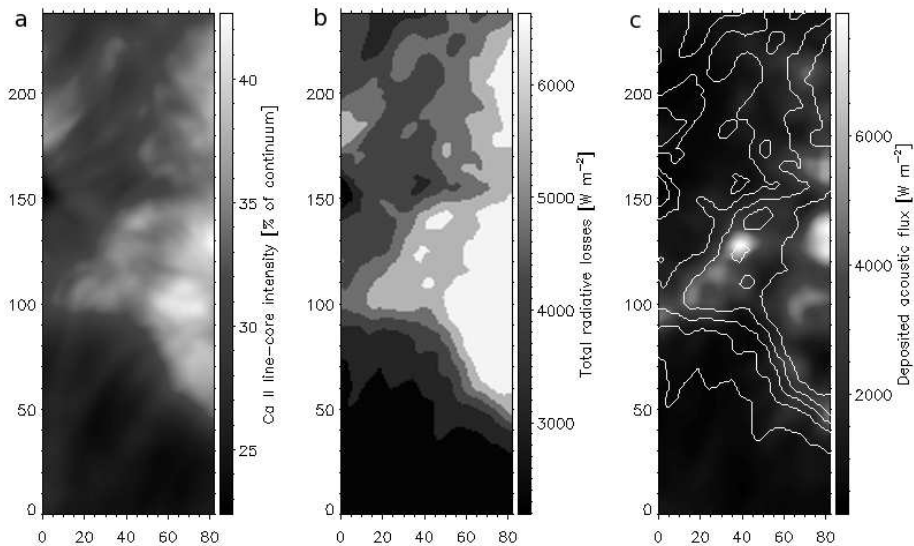


Figure 1: (a) Plage and quiet areas in the Ca II 854.2 nm line centre. (b) Map of total radiative losses. (c) Map of deposited acoustic flux with contours of the total radiative losses. The coordinates are in pixels (1 pix = 0.167 arcsec).

The energy flux $F_{\text{ac,tot}}$ transported by the (magneto)acoustic waves into the chromosphere can be derived from the spectral power density $P_v(\nu)$ of Doppler oscillations. According to Bello González *et al.* (2009),

$$F_{\text{ac,tot}} = \int_{\nu_{\text{ac}}}^{\infty} \rho P_v(\nu) v_{\text{gr}}(\nu) d\nu, \quad (1)$$

where the acoustic cutoff frequency $\nu_{\text{ac}} = \gamma g / (4\pi c_s) \cos \theta$ depends on the magnetic field inclination θ , ρ is a density taken from the model atmosphere, and $v_{\text{gr}} = c_s \sqrt{1 - (\nu_{\text{ac}}/\nu)^2}$ is the group velocity with which the energy is transported. The sound speed $c_s = \sqrt{\gamma p / \rho}$ of about 8 km s^{-1} is calculated using the pressure p and density ρ of the model. The energy deposited by acoustic flux at the formation height of the Ca II 854.2 nm line core, 900–1400 km, was computed as a difference of acoustic fluxes $F_{\text{ac,tot}}(1000 \text{ km}) - F_{\text{ac,tot}}(1400 \text{ km})$, calculated from Doppler velocities measured in the inner wings and the line centre, using gas parameters from the

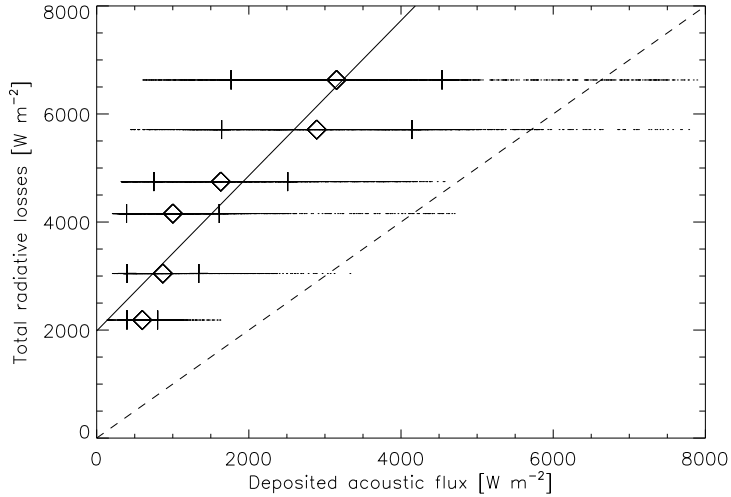


Figure 2: Total radiative losses versus deposited acoustic flux. Mean values (diamonds) and 1σ ranges of radiative losses are shown together with a linear fit. The dashed diagonal line represents the full coverage of radiative losses by acoustic flux.

models at corresponding heights, and magnetic field inclination obtained from the inversion of the line Fe I 617.3 nm. The resulting map of the deposited acoustic flux is shown in Fig. 1c. Note that since we measure only the line-of-sight component of the velocity oscillations, the spectral power densities $P_v(\nu)$ can be underestimated and the values of acoustic energy fluxes obtained from (1) should be considered as lower limits.

4. Discussion

It is seen from Fig. 1 that the deposited acoustic flux is indeed enhanced in the plage region. The coefficient of spatial correlation between the radiative losses and deposited acoustic flux is 70 %. However, there are many areas with high radiative losses where the acoustic flux is too small and vice versa. A scatter plot of radiative losses versus the deposited acoustic flux is displayed in Fig. 2 together with mean values and 1σ limits of the radiative losses. A linear fit to the mean values is also shown. The scatter of values

of the radiative losses is very large and the sampling by only six model atmospheres is too rough. A finer grid of models including semiempirical models of plages should be used in the future. These preliminary results demonstrate that the deposited acoustic flux provides at least 25–30 % of the energy radiated by the quiet chromosphere and 50 % of the energy emitted by plage regions. However, we have to keep in mind that our approach based on static semi-empirical models may skew the information on highly dynamical energy-transfer processes in the chromosphere.

Acknowledgements

This work was supported by the Czech Science Foundation under grants 14-04338S, P209/12/P568, P209/12/0287, and by the project RVO:67985815 of the Academy of Sciences of the Czech Republic.

References

- Bel, N. and Leroy, B.: 1977, *Astron. Astrophys.* **55**, 239.
- Bello González, N., Flores Soriano, M., Kneer, F., and Okunev, O.: 2009, *Astron. Astrophys.* **508**, 941.
- Cauzzi, G., Reardon, K. P., Uitenbroek, H., *et al.*: 2008, *Astron. Astrophys.* **480**, 515.
- Cavallini, F.: 2006, *Solar Phys.* **236**, 415.
- Garcia, A., Klvaňa, M., and Sobotka, M.: 2010, *Cent. Eur. Astrophys. Bull.* **34**, 47.
- Jefferies, S. M., McIntosh, S. W., Armstrong, J. D., *et al.*: 2006, *Astrophys. J.* **648**, L151.
- Rybicki, G. B. and Hummer, D. G.: 1992, *Astron. Astrophys.* **262**, 209.
- Sobotka, M., Švanda, M., Jurčák, J., *et al.*: 2013, *Astron. Astrophys.* **560**, A84.
- Stangalini, M., Del Moro, D., Berrilli, F., and Jefferies, S. M.: 2011, *Astron. Astrophys.* **534**, A65.
- Stix, M.: 2004, *The Sun: An Introduction*, Berlin: Springer, Chapter 9.4.
- Vernazza, J. E., Avrett, E. H., and Loeser, R.: 1981, *Astrophys. J., Suppl. Ser.* **45**, 635.